May 1984

LRP 236/84

OPTIMIZATION OF ANTENNAE FOR ALFVEN WAVE HEATING IN THE TCA TOKAMAK

F. Hofmann, K. Appert, L. Villard

ABSTRACT

A one-dimensional cylindrical model including Hall current effects is used to optimize the antenna system for Alfvén wave heating in the TCA tokamak. The power absorbed in the plasma is computed as a function of the shape of the antenna, its orientation with respect to the poloidal magnetic field, its radial position as well as its fundamental toroidal wave number. The study reveals several ways of improving the performance of the modular antenna system used in TCA.

1. INTRODUCTION

Resonant absorption of Alfvén waves has been proposed many years ago [1,2] as a possible candidate for heating tokamak plasma to fusion temperatures. The method is currently being investigated on serveral tokamaks [3,4,5]. Recent experiments on TCA, at RF power levels exceeding the ohmic heating power (200 kW), have shown substantial increases in electron and ion temperature [3]. Theoretical calculations [6] of absorbed power, using a 1-D cylindrical model including Hall currents have given good agreement with experimental results [7], as far as the excitation of modes with $m=\pm 1$ is concerned. Not all the observations, however, can be explained with the cylindrical model [8]. Some experimental features seem to be due to the toroidal geometry. Presently, the torus can only be modeled in ideal MHD, i.e. neglecting finite frequency (or Hall current) effects [9]. The two theoretical models are complementary but, in general, the cylindrical one compares better with the experiment. This gives us a certain confidence to use the 1-D model for antenna optimization.

Previous work in this direction [10] was mainly concerned with optimizing the antenna loading in ω-k space, using an ideal helical antenna with fixed current. Here, we develop the theory of a general single-mode antenna, modeled by an imposed current distribution with an arbitrary radial profile. Then, we consider a real antenna, similar to the one mounted in TCA, and we include the effects of feed currents. We examine various optimization criteria, and we investigate the effects of varying the toroidal wave number, the shape of the antenna, the tilt angle between the antenna current and the poloidal magnetic field, the radial positions of antenna and plasma surfaces and finally the geometry of the feed currents.

2. BASIC ANTENNA THEORY

The frequencies in the range of Alfvén wave heating are so small that the wave fields in the vacuum between plasma (radius r_p) and conducting wall (radius r_s) can be described by quasistationary electrodynamics. A straigthforward antenna theory can be developed if the antenna is modeled by imposed currents flowing in the vacuum and not as pieces of metal in which image currents can flow. It is our intention to treat antennae of realistic shapes. In the framework of a cylindrically symmetric model they can be described as sums of Fourier-modes, exp $i(m\theta+kz-\omega t)$ [11], where r, θ an z are the usual cylindrical coordinates. In this section we discuss the theory of one single mode.

The antenna geometry is chosen as follows. Surface currents are allowed to flow on radii r_1 and r_2, with $r_p<r_1<r_2<r_s$. The radius r_2 will eventually tend towards r_s. In the range $r_1\leq r\leq r_2$ volume currents may flow. These currents are necessary to describe the currents in the feeders of a realistic antenna [10].

In quasistationary electrodynamics the current density, j, must satisfy

$$\nabla\cdot\vec{j} = 0 \tag{1}$$

and may therefore be written as

$$\vec{j} = \nabla \times \vec{b} \tag{2}$$

where $\vec{b}$ is an arbitrary "current potential". In cylindrical coordinates, $\nabla\times\vec{b}$ contains radial derivatives of b_θ and b_z, but not of b_r. The current potential b can therefore have the form

$$\left.\begin{aligned} b_r &= i\alpha_r(r) - i\beta\,\delta(r-r_1) + i\gamma\,\delta(r-r_2) \\ b_\theta &= \alpha_\theta(r) \\ b_z &= \alpha_z(r) \end{aligned}\right\} \tag{3}$$

The potential $\vec{b}$ is zero if $r<r_1$ or $r>r_2$. The quantities β and γ are arbitrary constants and $\vec{\alpha}(r)=(i\alpha_r,\alpha_\theta,\alpha_z)$ is an arbitrary vector function. Upon substituting eq. (3) into eq. (2) we obtain

$$\left.\begin{aligned} j_r &= \frac{im}{r}\alpha_z - ik\alpha_\theta \\ j_\theta &= -k\alpha_r - \alpha_z' + (k\beta - \alpha_z)\,\delta(r-r_1) - (k\gamma - \alpha_z)\,\delta(r-r_2) \\ j_z &= \frac{1}{r}(r\alpha_\theta)' + \frac{m}{r}\alpha_r - \left(\frac{m}{r}\beta - \alpha_\theta\right)\delta(r-r_1) + \left(\frac{m}{r}\gamma - \alpha_\theta\right)\delta(r-r_2) \end{aligned}\right\} \quad (4)$$

Here the prime denotes $\partial/\partial r$.

Any antenna configuration with two surface currents at $r=r_1$ and $r=r_2$ can be obtained from a special choice of $\alpha(r)$, β and γ. Let us mention two simple examples. With $\alpha=\gamma=0$ a helical antenna at $r=r_1$ without feeders is obtained. The choice $\alpha_r=\alpha_z=0$ and $r\alpha_\theta=m\beta=m\gamma$ leads to an antenna with poloidal surface currents (j_θ) at $r=r_1$ and r_2 and radial feed currents (j_r).

The wave equation in vacuum is

$$\nabla \times \vec{B} = \mu_0 \vec{j} \quad (5)$$

Defining a magnetic field potential, ϕ, by

$$\vec{B} = \mu_0 (\vec{\alpha} - \nabla\phi) \quad (6)$$

we can write the wave equation (5) restricted to the regions $r_p<r<r_1$, $r_1<r<r_2$ and $r_2<r<r_s$ as

$$\Delta\phi = \nabla \cdot \vec{\alpha} \quad (7)$$

The boundary and matching conditions are

$$\left.\begin{aligned} &\phi'(r_s) = 0 \\ &[\![\phi]\!]_{r_2} = i\gamma\,, \quad [\![\phi']\!]_{r_2} = -\alpha_r(r_2) \\ &[\![\phi]\!]_{r_1} = -i\beta\,, \quad [\![\phi']\!]_{r_1} = \alpha_r(r_1) \end{aligned}\right\} \quad (8)$$

The bracket $[\![\phi]\!]$ denotes the jump $\phi(r+0)-\phi(r-0)$. If $r_2 \to r_s$ we have $\phi'(r_2+0)\to 0$ and therefore $\phi'(r_s)=\alpha_r(r_s)$. This is the situation where the surface current at $r=r_1$ is fed from outside.

Here we do not specify the boundary conditions at the plasma-vacuum interface as we do not discuss the solution of the wave equation in the plasma. For this part of the problem the reader is referred to a recent publication [12]. It is easy to solve eqs. (7) and (8) numerically whith a Runge-Kutta procedure.

Once the magnetic fields or ϕ are known one can calculate the power emitted by the antenna. Let us define the complex power emitted per unit area of the inner antenna sheet :

$$\frac{P}{A} = -\frac{1}{2r_1}\int \vec{j}\cdot\vec{E}^{*}\, r\,dr \qquad (9)$$

Using eq. (2) and Maxwell's equations one has

$$\frac{P}{A} = \frac{i\omega}{2r_1}\int_{r_1}^{r_2} \vec{A}\cdot\vec{B}^{*}\, r\,dr + \frac{\omega}{2r_1}\left[\beta r_1 B_r^{*}(r_1) - \gamma r_2 B_r^{*}(r_2)\right] \qquad (10)$$

In the following sections we will always choose $r_2=r_S$ and we define $r_A=r_1$ as the antenna radius. The currents flowing at $r_2=r_S$ are dissipationless.

3. FOURIER EXPANSION OF REALISTIC ANTENNA CURRENTS

Arbitrary antenna currents, at $r=r_A$, may be written as

$$j_\theta = \sum_{k,m} S_{\theta_{k,m}}\, \delta(r-r_A)\, e^{i(m\theta+kz-\omega t)} \qquad (11)$$

$$j_z = \sum_{k,m} S_{z_{k,m}}\, \delta(r-r_A)\, e^{i(m\theta+kz-\omega t)} \qquad (12)$$

In applying this formalism to a torus, we replace kz by $n\phi$ where n is the toroidal wave number, $n=kR$, ϕ is the toroidal angle, $\phi=z/R$, and R is the major radius. Integrating $\nabla\cdot\vec{j}=0$ from $r=r_A-\varepsilon$ to $r=r_A+\varepsilon$ where $\varepsilon \to 0$, and assuming $\vec{j}=0$ for $r<r_A$ gives us the radial component of the feed current at $r=r_A$,

$$\left[j_{r_{n,m}}\right]_{r=r_A} = -i\left[\frac{m}{r_A} S_{\theta_{n,m}} + \frac{n}{R} S_{z_{n,m}}\right] e^{i(m\theta+n\varphi-\omega t)} \qquad (13)$$

If we then write, for $r>r_A$,

$$j_{r_{n,m}}(r) = j_{r_{n,m}}(r_A)\ V_{n,m}(r) \tag{14}$$

where $V_{n,m}(r_A)=1$, and if we assume $j_z=0$ for $r>r_A$, we can express the feed currents as

$$j_{r_{n,m}} = -i\left[\frac{m}{r_A} S_{\theta_{n,m}} + \frac{n}{R} S_{z_{n,m}}\right] V_{n,m}(r)\, e^{i(m\theta+n\varphi-\omega t)} \tag{15}$$

$$j_{\theta_{n,m}} = \left[\frac{1}{r_A} S_{\theta_{n,m}} + \frac{n}{mR} S_{z_{n,m}}\right] \frac{\partial}{\partial r}(r V_{n,m})\, e^{i(m\theta+n\varphi-\omega t)} \tag{16}$$

Comparing eqs (15) and (16) with eq. (4) we find that $\beta=S_\theta/k$, $\alpha_r=-(r\alpha_\theta)'/m$, $\alpha_\theta=(mS_\theta/kr_A+S_z)V$ and $\alpha_z=0$. As an example, let us compute the functions $S_{\theta_{n,m}}$, $S_{z_{n,m}}$ and $V_{n,m}$ for the TCA antenna in standard phasing (Fig. 1). In this case, the antenna currents at $r=r_A$ are given by

$$\left.\begin{aligned} j_\theta &= \frac{I}{w}\,\delta(r-r_A)\, f(\theta,\varphi)\, e^{-i\omega t} \\ j_z &= 0 \end{aligned}\right\} \tag{17}$$

where w is the width of the antenna, $w=2R\,\varphi_A$. The function $f(\theta,\varphi)=\pm1$ within the rectangular surfaces shown in Fig. 1, and $f(\theta,\varphi)=0$ elsewhere ($f=1$ for $I>0$ and $f=-1$ for $I<0$). $f(\theta,\varphi)$ is expanded as

$$f(\theta,\varphi) = \sum_{n,m} c_{n,m}\, e^{i(m\theta+n\varphi)} \tag{18}$$

and the coefficients $c_{n,m}$ are given by

$$c_{n,m} = \frac{1}{4\pi^2} \int_{-\pi}^{\pi} d\theta \int_{-\pi}^{\pi} d\varphi\, f(\theta,\varphi)\, e^{-i(m\theta+n\varphi)} \tag{19}$$

It follows that

$$S_{\theta_{n,m}} = \frac{I}{w} c_{n,m} \quad , \quad S_z = 0 \, .$$

Evaluation of the integral (19) yields

$$S_{\theta_{n,m}} = \frac{\delta I}{\pi^2 W} \frac{\sin m\theta_A}{m} \frac{\sin n\varphi_A}{n} \tag{20}$$

where m=odd and n=±2,±6,±10 ... The function $V_{n,m}(r)$ depends on the geometry of the feed currents. We shall consider two cases : a) purely radial feed currents and b) vertical feed currents (as in TCA).In case a) we have, for $r>r_A$

$$j_{\theta_{n,m}} = 0 \ , \ \frac{\partial}{\partial r}(r V_{n,m}) = 0 \ , \ V_{n,m} = \frac{r_A}{r} \tag{21}$$

In case b), things are more complicated. Consider a poloidal section of the antenna at $\varphi=0$ (Fig. 2). The feed currents can be written as

$$j_r = \frac{I}{W r_F} g(\theta,\varphi) \ , \ j_\theta = -\tan\theta \ j_r \ , \ j_z = 0 . \tag{22}$$

where the function $g(\theta,\varphi)$ is given by

$$g(\theta,\varphi) = h(\theta) H(\varphi) \tag{23}$$

and $h(\theta)$ and $H(\varphi)$ are defined by

$$h(\theta) = \delta(\theta-\theta_F) + \delta(\theta-\pi+\theta_F) - \delta(\theta+\theta_F) - \delta(\theta-\pi-\theta_F) \tag{24}$$

$$\left.\begin{aligned} &H(\varphi)=1 \quad \text{for } -\varphi_A<\varphi<\varphi_A \text{ and } \pi-\varphi_A<\varphi<\pi+\varphi_A \\ &H(\varphi)=-1 \quad \text{for } \tfrac{\pi}{2}-\varphi_A<\varphi<\tfrac{\pi}{2}+\varphi_A \text{ and } \tfrac{3\pi}{2}-\varphi_A<\varphi<\tfrac{3\pi}{2}+\varphi_A \\ &H(\varphi)=0 \quad \text{elsewhere} \end{aligned}\right\} \tag{25}$$

Note that θ_F is a function of r_F, θ_F=arc tan(X_F/r_F) (Fig. 2). The function $g(\theta,\varphi)$ is expanded as

$$g(\theta,\varphi) = \sum_{n,m} d_{n,m} e^{i(m\theta+n\varphi)} \tag{26}$$

and the coefficients $d_{n,m}$ are evaluated according to eq. (19),

$$d_{n,m} = -\frac{8i}{\pi^2 n} \sin m\theta_F \sin n\varphi_A \tag{27}$$

where m=odd and n=±2,±6,±10 ... It follows that

$$j_r = \frac{-8iI}{\pi^2 w r_F} \sum_{n,m} \frac{\sin n\varphi_A}{n} \sin m\theta_F \, e^{i(m\theta + n\varphi - \omega t)} \tag{28}$$

and by comparing with eq. (15) we find

$$V_{n,m}(r) = \frac{r_A}{r} \frac{\sin m\theta_F}{\sin m\theta_A} \tag{29}$$

$$\frac{\partial}{\partial r}(r V_{n,m}) = -\frac{m r_A}{r} \tan\theta_F \frac{\cos m\theta_F}{\sin m\theta_A} \tag{30}$$

4. OPTIMIZATION CRITERIA AND BASIC ASSUMPTIONS

In optimizing an RF heating system, one obviously wishes to maximize the power transferred to the plasma, while minimizing antenna voltage, antenna surface area and resistive losses. The trade-off between voltage, surface area and resistive losses, however, is not at all obvious and depends on many parameters. If, for example, the antennae are unshielded, the voltage must be kept low in order to avoid arcing. If on the other hand the antennae are enclosed in Faraday screens, a small surface area is probably more important than low voltage.

In order to limit the number of parameters to be varied, we make the following assumptions : The total antenna surface area is fixed at 16 % of the plasma surface. We consider only M=1 excitation with two antennae on a poloidal circumference, dephased by 180 ° (M and N define the excitation structure, i.e. the geometry and phasing of the various antennae, whereas m and n define a particular mode or Fourier component). We assume that there are a total number of 4N antennae in the torus, where N is the lowest toroidal wave number. The phase angle between two adjacent antennae on a toroidal circumference is always

180 °. We only consider rectangular or trapezoidal antennae with vertical or radial feed currents. In most of the calculations we assume that the frequency is just beyond the edge of the second continuum of the lowest n (usually n=2). In the case of a purely poloidal antenna, this implies that about half the power is deposited in the center and the other half close to the edge of the plasma. We generally assume $\omega/\omega_{ci}=0.217$. This corresponds to present TCA conditions in deuterium (ν=2.5 MHz, B=1.5 T). When N is varied, however, ω and ω/ω_{ci} are assumed to increase with N in such a way that the plasma density on the continuum edge remains constant. Standard values of antenna and shell radii are $r_A/a=1.15$ and $r_S/a=1.5$, except when these quantities are varied (section 8). All calculations are based on a standard tokamak equilibrium with $q_0=0.91$, $q_a=3.27$, $j=j_0(1-(r/a)^2)^{2.6}$, $\rho=\rho_0(1-(r/a)^2)$. The plasma aspect ratio is taken as R/a=3.3, except when a is varied, in which case R=const.

Under these conditions, we compute the power transferred to the plasma, in cylindrical approximation, eq. (10), as a function of the following parameters : 1) toroidal wave number, N, 2) antenna length to width ratio, 3) antenna tilt angle with respect to the poloidal magnetic field, 4) antenna radial position, 5) plasma radius, and 6) geometry of feed currents. Results are presented in the sections below.

5. LOW vs. HIGH TOROIDAL WAVE NUMBERS

One of the important parameters in an Alfvén wave heating system is the toroidal wave number, N, of the fundamental mode to be excited. The choice of N not only determines the geometry of the antenna system but also fixes the optimum excitation frequency for a given plasma density. The basic question is whether low or high N's should be preferred. In order to answer this question, we compare systems with different N's, under the following assumptions : the number of antennae in the torus, N_A, is assumed proportional to N ($N_A=4N$). The total antenna surface area and the length of each antenna are held constant, whereas the antenna width is proportional to 1/N. The RF current per antenna also varies as 1/N, in order to

keep the current density constant. The excitation frequency is assumed to increase with N in such a way that the (n=-N, m=-1) continuum edge always corresponds to the same value of the plasma density. Under these conditions, we compute the total power absorbed in the plasma for various N's. The result is shown in Fig. 3, where we plot absorbed power as a function of the normalized frequency ($\Omega=(\omega a/B_0)\sqrt{\mu_0\rho_0}$). In Fig. 4 we show the absorbed power on the edge of the (n=-N, m=-1) continuum as a function of N. We observe a clear maximum in the neighbourhood of N=4.Higher N numbers do not seem to be attractive, even in the cylindrical approximation. In toroidal geometry, high-N excitation leads to the additional problem of power deposition near the edge, due to mode coupling [9]. Also plotted in Fig. 4 is the antenna terminal voltage as a function of N.

It should be remembered that the results presented in Fig. 4 were obtained assuming constant current density in the antennae. If we assume constant terminal voltage or constant resistive losses, the maximum is shifted towards slightly lower values of N (i.e. N=3). On the other hand, if we decrease the plasma-wall spacing (e.g. $r_s/a=1.2$) or if we increase the aspect ratio (e.g. R/a=4.3), the optimum N is shifted upwards to values between 6 and 8.

6. OPTIMUM SHAPE OF A RECTANGULAR POLOIDAL ANTENNA

The simplest modular antenna system for excitation of Alfvén waves in a tokamak is the rectangular poloidal antenna (Fig. 1). If the total antenna surface is fixed, the only free parameter is the length-to-width ratio, θ_A/φ_A. (Length and width of a poloidal antenna are given by $2\, r_A\theta_A$ and $2\, R\varphi_A$, respectively). In this section, we compute the absorbed power as a function of the angle θ_A, assuming $\theta_A\varphi_A$=const. The calculations were done for a TCA-type system with 8 antennae in N=2,M=1 phasing. The excitation frequency and plasma density are fixed (Ω=1). The results are shown in Fig. 5. When the current in each antenna is kept constant, the power increases roughly linearly with θ_A. From this result one might conclude that θ_A should be made as large as possible. However, when the voltage on the antenna terminals is kept constant, the trend is exactly opposite and the absorbed power varies approximately as $\theta_A^{-3/2}$.

We believe that low voltage is much more important than low current, at least for unshielded antennae [13]. In TCA, for example, the absorbed power could be increased by a factor 3, without changing the antenna voltage, if the angle θ_A were reduced to 22.5 °. Such a modification would, however, pose some problems with diagnostic access, since the toroidal angle, φ_A, would be increased by a factor 2, and the toroidal coverage would be 61 %. In Fig. 5, we also show the case where the resistive losses, $D \sim I^2(\theta_A/\varphi_A)$, are assumed constant. In this case, I varies as θ_A^{-1} and the absorbed power becomes almost independent of θ_A. In conclusion, it appears that an unshielded poloidal antenna should be made as short and wide as possible in order to minimize the voltage on the terminals.

7. SEGMENTED HELICAL ANTENNA

Up to this point, we have been considering purely poloidal antennae. These excite modes with positive and negative helicity, leading to a non-optimal power deposition profile (typically one half in the center and one half on the edge). In order to avoid edge loading, one might consider using a continuous helical antenna. However, this is not a very attractive solution from a practical point of view. Here, we wish to investigate the performance of a modular helical antenna, consisting of short helical segments. Let us consider a tilted trapezoidal antenna, as shown in Fig. 6. The parameter t defines the tilt angle, $t = d\varphi/d\theta$. Fourier expansion of the surface currents, according to eqs (11) and (12) yields

$$S^t_{\theta_{n,m}} = \frac{4I}{\pi^2 R \varphi_A} \frac{\sin n\varphi_A}{n} \frac{\sin(m+tn)\theta_A}{m+tn} \tag{31}$$

$$S^t_{z_{n,m}} = \frac{Rt}{r_A} S^t_{\theta_{n,m}} \tag{32}$$

where m=odd and n=±2,±6,±10 ... Similarly, the Fourier expansion of the vertical feed currents leads to

$$V^t_{n,m}(r) = \frac{r_A}{r} \frac{\sin(m\theta_F + tn\theta_A)}{\sin(m+tn)\theta_A} \tag{33}$$

$$\frac{\partial}{\partial r}\left(r V^{t}_{n,m}\right) = -\frac{m r_A}{r}\,\frac{\cos(m\theta_F + t n \theta_A)}{\sin(m+tn)\theta_A}\,\tan\theta_F \qquad (34)$$

where we have used eqs (15) and (16) to describe the volume currents in the vacuum, for $r_A<r<r_S$. It is obvious that the excitation amplitude, $S^{t}_{\theta_{n,m}}$ (eq. 31) now depends on the relative signs of m and n, i.e. on the helicity of the mode considered.

Fig. 7 shows two typical loading curves, for TCA parameters, one with positive, the other with negative tilt. We note that the two curves are completely different although the tilt angle used here, t=0.2, is much smaller than that which would be required for aligning the antennae with a (n=2, m=1) helix, i.e. t=m/n=0.5. This indicates that preferential excitation of modes with positive or negative helicity is possible with moderately tilted antennae. In Fig. 8 we show how the total absorbed power is split up between modes with positive and negative helicity. The Figure displays the fractional loading due to these modes as a function of the tilt parameter, t. The frequency is chosen just beyond the edge of the (n=-2, m=-1) continuum (Ω=0.925). We note that for t=±0.3, the plasma responds as if it were excited with a perfect helical antenna. Even for t=±0.1, corresponding to a physical tilt angle of α=arc tan(tR/a)=18°, there is only 17% of the power in the unwanted modes. We conclude that efficient mode selection and, hence, power deposition profile optimization can be achieved by using a segmented helical antenna. Such an antenna may, however, lead to other problems : since it produces an electric field component parallel to the toroidal magnetic field, a Faraday screen may turn out to be necessary.

8. EFFECT OF PLASMA AND ANTENNA RADII ON ABSORBED POWER

It is clear that, in order to optimize the power transferred to the plasma, the antenna should be placed as close to the plasma as possible and the conducting shell should be as far away as possible. Starting from TCA conditions, (r_A/a=1.15, r_S/a=1.5) we first consider the effect of varying either the antenna radius or the plasma radius (Fig. 9). Plasma density, q-profile and excitation frequency are assumed constant. On the left-hand side of Fig. 9, we show the

power as a function of plasma radius, with fixed antenna radius. The slope of this curve agrees well with measurements in TCA [14]. On the right-hand side of the same Figure we plot the power as a function of antenna radius, with fixed plasma radius. We note that if one wishes to increase the distance between plasma and antenna (e.g. in order to introduce a Faraday screen) while minimizing the associated loss of coupling, then it is preferable to reduce the plasma radius rather than increase the antenna radius. This is seen more clearly in Fig. 10 where we plot the loading as a function of a/r_S for various values of Δ, where $\Delta=(r_A-a)/r_S$. It is interesting to note that the absorbed power reaches its maximum for relatively small values of a/r_S.

9. COMPARISON BETWEEN RADIAL AND VERTICAL FEED CURRENTS

All the results presented so far were obtained by assuming vertical currents feeding the antennae (see section 3). When the feed currents are purely radial, the area enclosed by the antenna loop is increased and the coupling to the plasma is improved. This is seen in Fig. 11 where we show the resistive loading as a function of Ω for the two cases with vertical and radial feed currents.

10. CONCLUSIONS

Two important conclusions can be drawn from the results presented above : firstly, we have shown that in a tokamak with small aspect ratio ($R/a = 3.3$), circular cross section and relatively large wall radius ($r_S/a=1.5$), the optimum toroidal wave number, N, for Alfvén wave heating is between 3 and 4. Both very low and very high N's lead to a considerable reduction in the power transferred to the plasma. If the aspect ratio is increased and the wall radius decreased (e.g. $R/a=4.3$, $r_S/a=1.2$) we obtain qualitatively the same result, but the optimum N is shifted to values between 6 and 8.

Secondly, by analyzing a modular helical antenna consisting of short segments which are tilted with respect to the poloidal magnetic field, we have demonstrated that almost pure helical modes can be

excited by using tilt angles which are only about one half of those corresponding to the helix of the mode. This implies that the optimization of the power deposition profile, and in particular, the elimination of power absorption near the edge of the plasma, are feasible without using a continuous helical antenna.

11. ACKNOWLEDGEMENTS

The authors wish to acknowledge fruitful discussions with Drs G.A. Collins, Ch. Hollenstein, R. Keller, A. Lietti, J.B. Lister, F.B. Marcus, A. Pochelon, J. Vaclavik and Prof. F. Troyon.

12. REFERENCES

[1] Grossmann, W., Tataronis, J., Z. Phys. 261 (1973) 217

[2] Hasegawa, A., Chen, L., Phys. Rev. Lett. 32 (1974) 454

[3] Behn, R., De Chambrier, A., Collins, G.A., Duperrex, P.-A., Heym, A., Hofmann, F., Hollenstein, Ch., Joye, B., Keller, R., Lietti, A., Lister, J.B., Moret, J.-M., Nowak, S., O'Rourke, J., Pochelon, A., and Simm, W., Plasma Physics and Controlled Fusion 26, 1A (1984) 173

[4] Bengtson, R.D., Evans, T.E., Li, Y.M., Mahajan, S.M., Oakes, M.E., Ross, D.W., Surko, C.M., Valanju, P.M., Wang, X.Z., and Watkins, J.G., 4th Int. Symp. on Heating in Toroidal Plasmas, Rome 21-28 March 1984

[5] Cross, R.C., Blackwell, B.D., Brennan, M.H., Borg, G., and Lehane, J.A., Proc. 3rd Joint Varenna-Grenoble Int. Symp. on Heating in Toroidal Plasmas, EUR 7979 EN (1982) Vol. I, 173

[6] Appert, K., and Vaclavik, J., Plasma Physics 25 (1983) 551

[7] Appert, K., Behn, R., De Chambrier, A., Collins, G.A., Duperrex, P.-A., Hofmann, F., Hollenstein, Ch., Joye, B., Keller, R., Lietti, A., Lister, J.B., O'Rourke, J., Pochelon, A., Simm, W., and Villard, L., Proc. 11th Europ. Conf. on Contr. Fusion and Plasma Phys., Aachen 1983, Part.I, p. 301 in Europ. Conf. Abstracts, Vol. 7D

[8] Appert K., De Chambrier, A., Collins, G.A., Duperrex, P.-A., Heym, A., Hofmann, F., Hollenstein, Ch., Joye, B., Keller, R., Lietti, A., Lister, J.B., Marcus, F.B., Moret, J.-M., Nowak, S., Pochelon, A., and Simm, W., 4th Int. Symp. on Heating in Toroidal Plasmas, Rome 21-28 March 1984

[9] Appert, K., Balet, B., Gruber, R., Troyon, F., Tsunematsu, T., and Vaclavik, J., Nuclear Fusion 22 (1982) 903

[10] Balet, B., Appert, K., and Vaclavik, J., Plasma Physics 24 (1982) 1005

[11] Michie, R.B., and Ross, D.W., 5th Topical Conf. on RF Heating in Plasmas, Madison, Wisconsin, February 1983

[12] Appert, K., Vaclavik, J., and Villard, L., Phys. Fluids 27 (1984) 432

[13] De Chambrier, A., Collins, G.A., Duperrex, P.-A., Heym, A., Hofmann, F., Hollenstein, Ch., Joye, B., Keller, R., Lietti, A., Lister, J.B., Marcus, F.B., Moret, J.M., Nowak, S., Pochelon, A., Simm, W., and Veprek, S., 4th Int. Symp. on Heating in Toroidal Plasmas, Rome 21-28 March 1984, invited paper

[14] De Chambrier, A., Cheetham, A.D., Heym, A., Hofmann, F., Joye, B., Keller, R., Lietti, A., Lister, J.B., Pochelon, A., Simm, W., Toninato, J.L., Tuszel, A., Proc. 3rd Joint Varenna-Grenoble Int. Symp. on Heating in Toroidal Plasmas EUR 7979 EN (1982) Vol. I, 161

FIGURE CAPTIONS

Fig. 1. Rectangular poloidal antenna (same as TCA)

Fig. 2. Poloidal section of antenna with vertical feed currents

Fig. 3. Absorbed power vs. $\Omega=(\omega a/B_0)\sqrt{\mu_0\rho_0}$ for N=2,4,6,8

Fig. 4. Absorbed power and antenna voltage on the edge of the (n=-N, m=-1) continuum vs. N

Fig. 5. Absorbed power vs. antenna length, assuming constant antenna surface

Fig. 6. Tilted trapezoidal antenna

Fig. 7. Resistive antenna load vs.Ω for two different tilt angles

Fig. 8. Fractional load for modes with positive and negative helicity vs. tilt angle (Ω=0.925)

Fig. 9. Absorbed power as a function of plasma radius and as a function of antenna radius

Fig. 10. Absorbed power vs. plasma radius for various values of the radial distance (Δ) between plasma and antenna

Fig. 11. Resistive antenna load vs. Ω, assuming vertical or radial feed currents

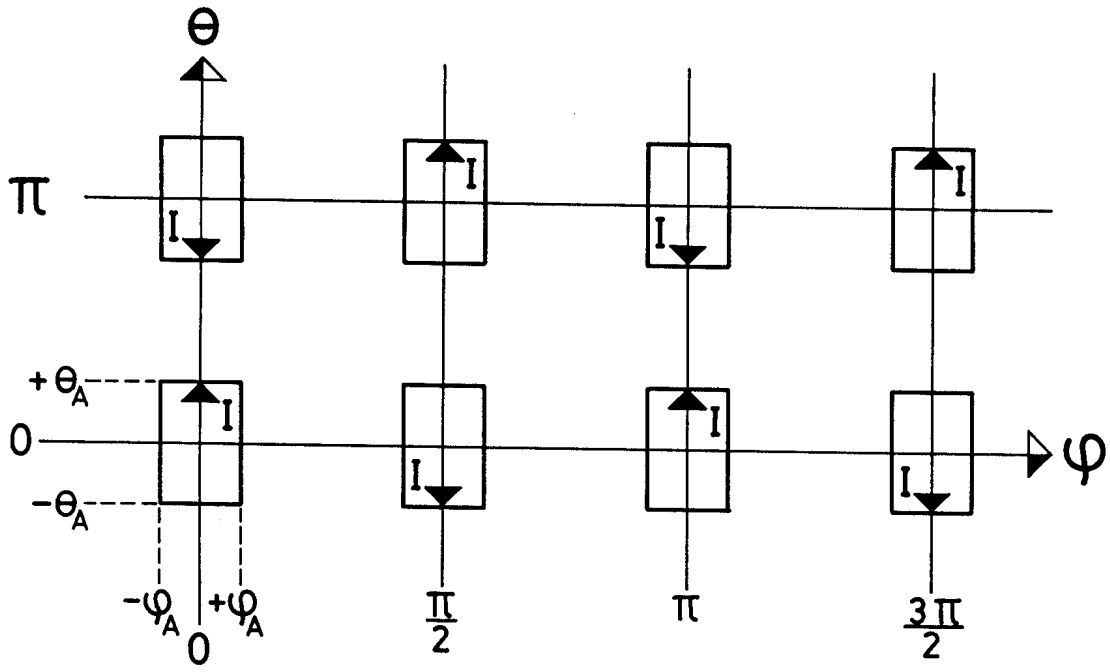

FIG. 1

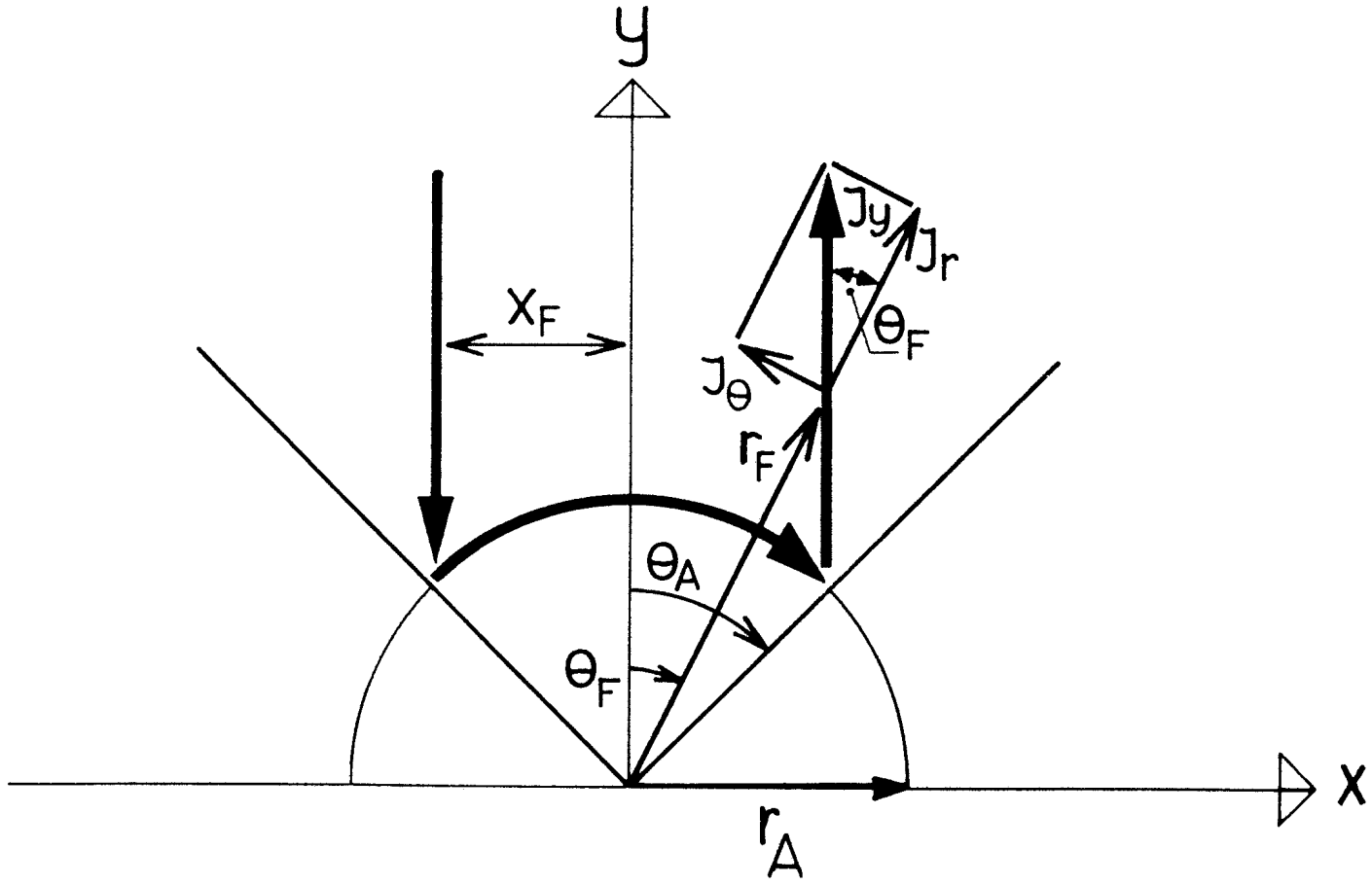

FIG. 2

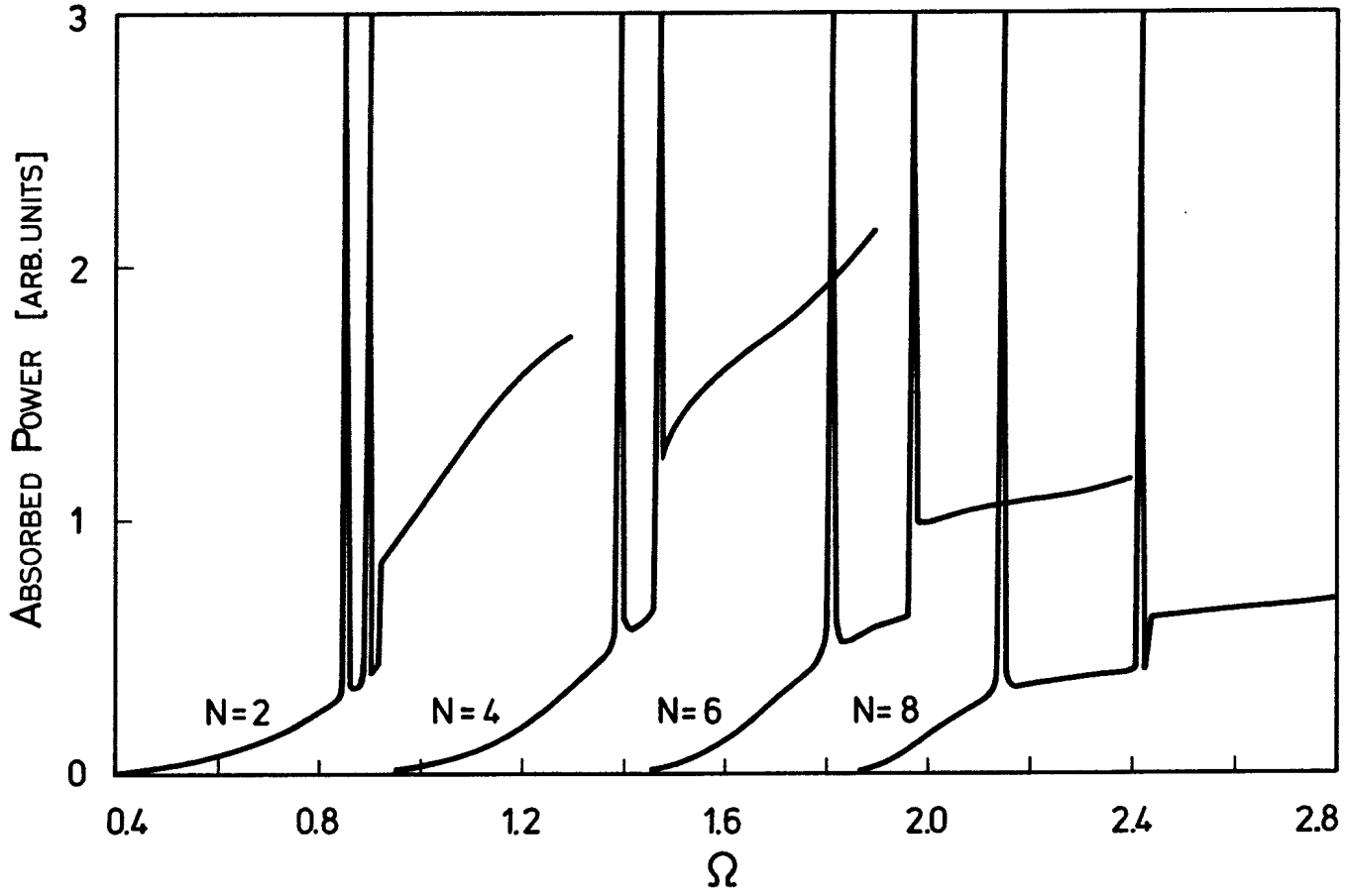

FIG. 3

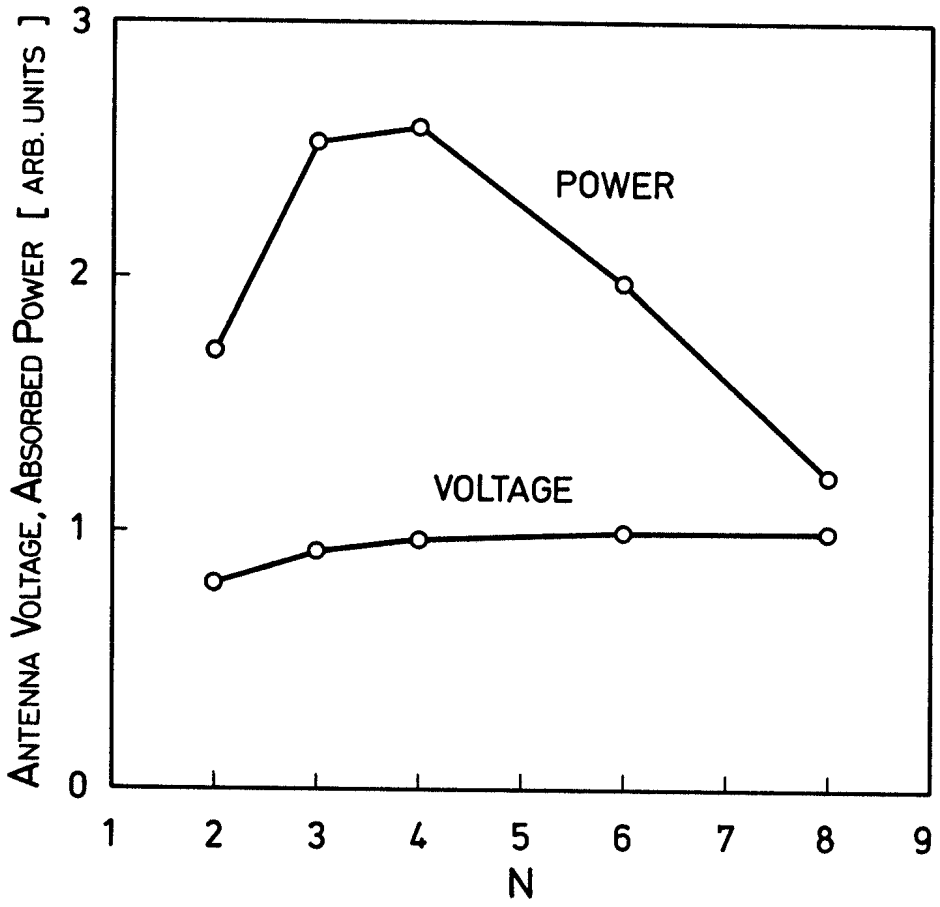
ANTENNA VOLTAGE, ABSORBED POWER [ARB. UNITS]
3
2
1
0
POWER
VOLTAGE
1
2
3
4
5
6
7
8
9
N

FIG. 4

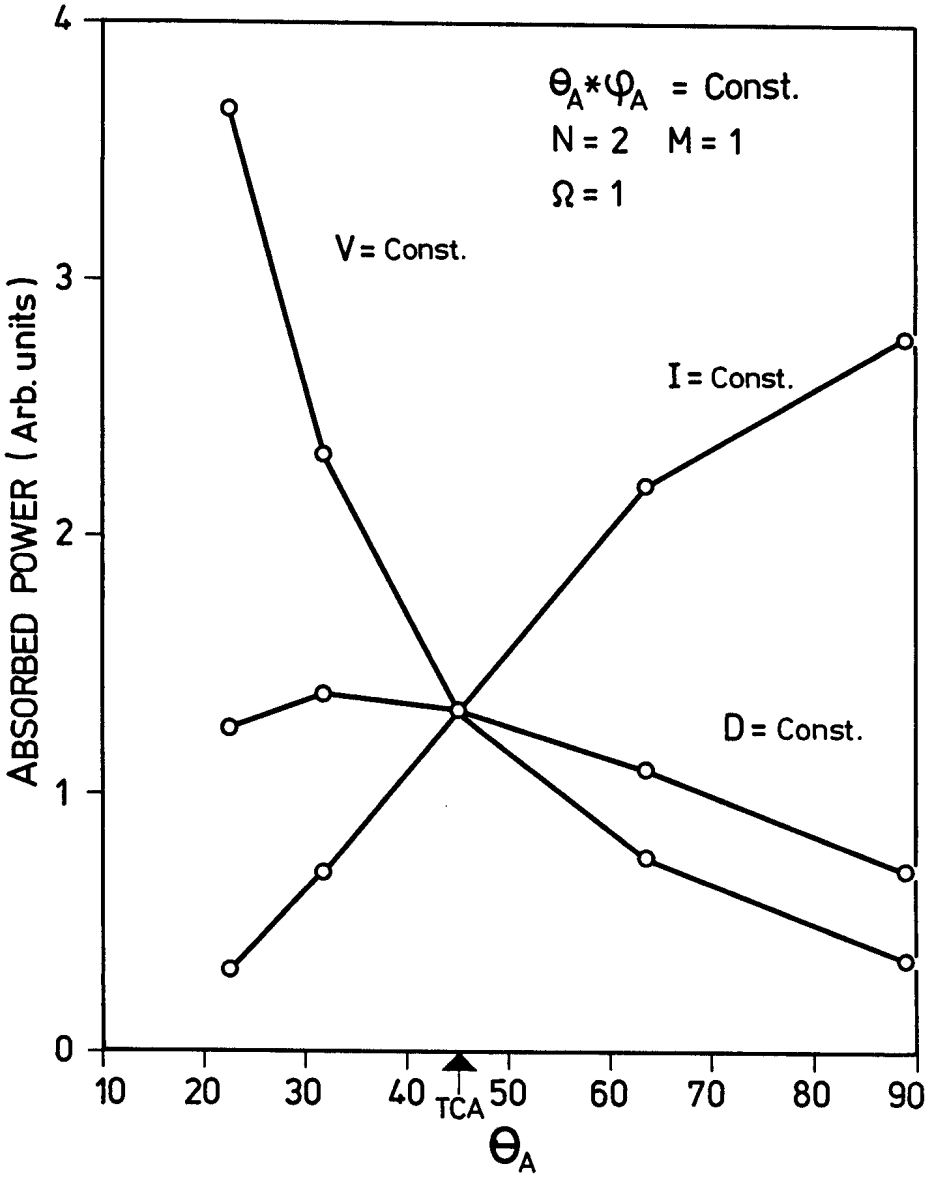
4
3
2
1
0
ABSORBED POWER (Arb. units)
$\theta_A * \varphi_A$ = Const.
N = 2 M = 1
Ω = 1
V = Const.
I = Const.
D = Const.
10
20
30
40
TCA
50
60
70
80
90
θ_A

FIG. 5

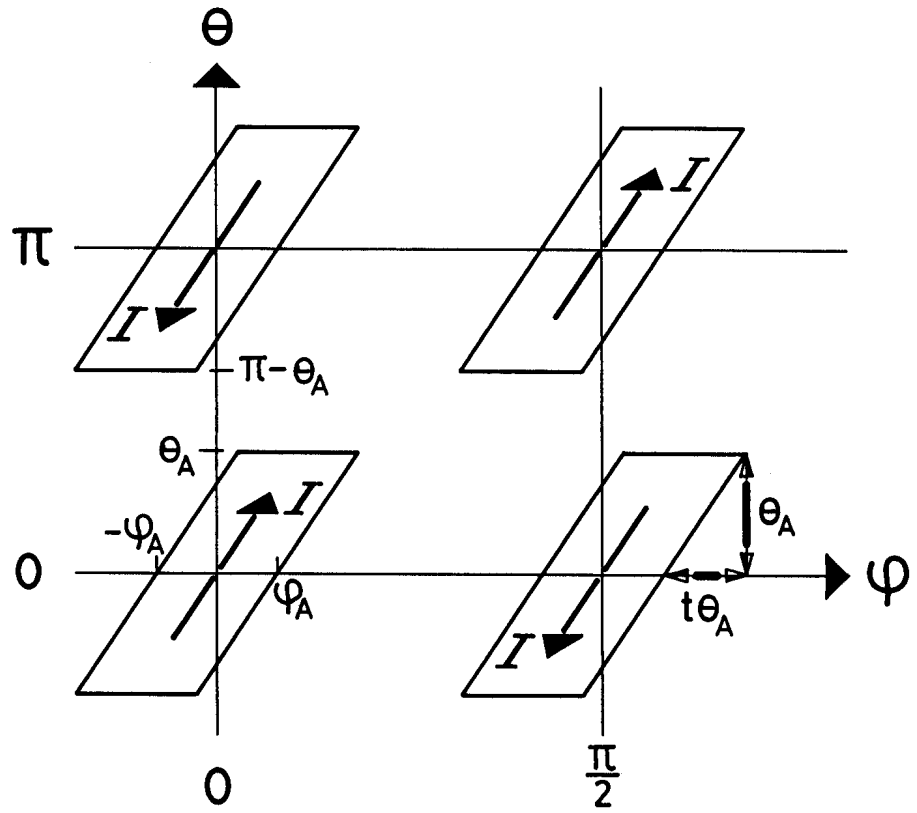

FIG. 6

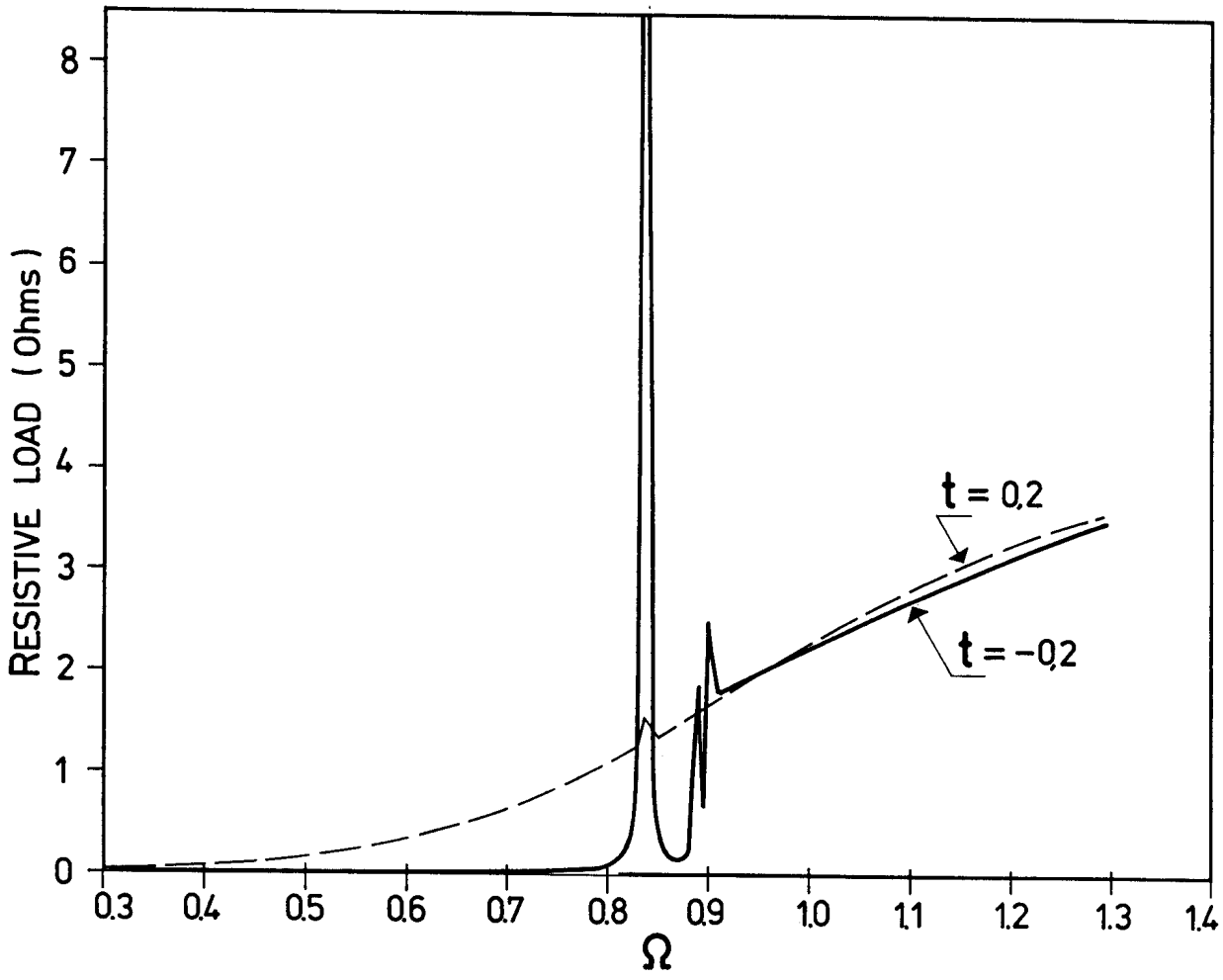
RESISTIVE LOAD (Ohms)
8
7
6
5
4
3
2
1
0
0.3
0.4
0.5
0.6
0.7
0.8
0.9
1.0
1.1
1.2
1.3
1.4
Ω
t = 0,2
t = -0,2

FIG. 7

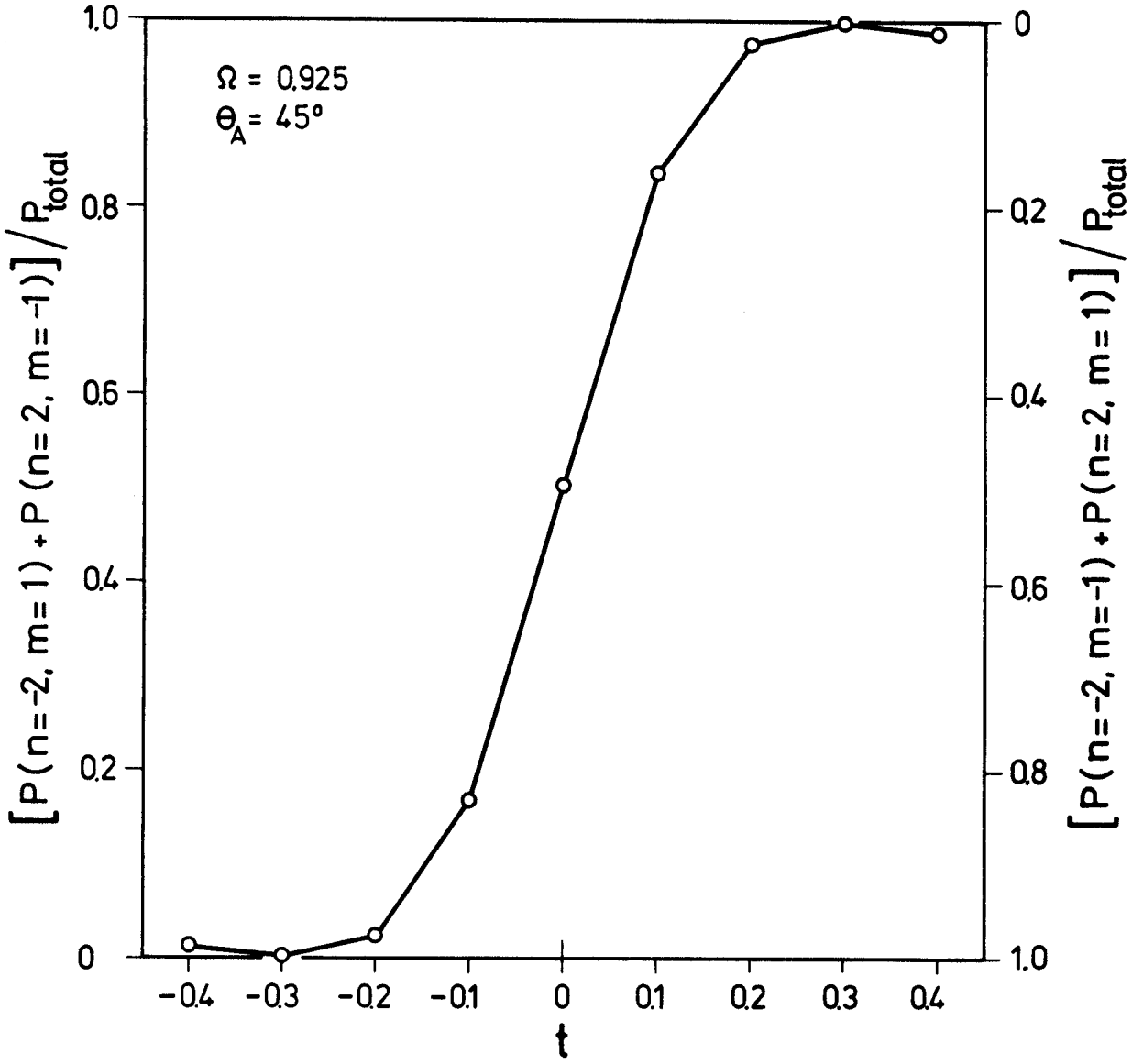
Ω = 0.925
θA = 45°
[P(n=-2, m=1) + P(n=2, m=-1)] / Ptotal
[P(n=-2, m=-1) + P(n=2, m=1)] / Ptotal
1.0
0.8
0.6
0.4
0.2
0
0
0.2
0.4
0.6
0.8
1.0
-0.4
-0.3
-0.2
-0.1
0
0.1
0.2
0.3
0.4
t

FIG. 8

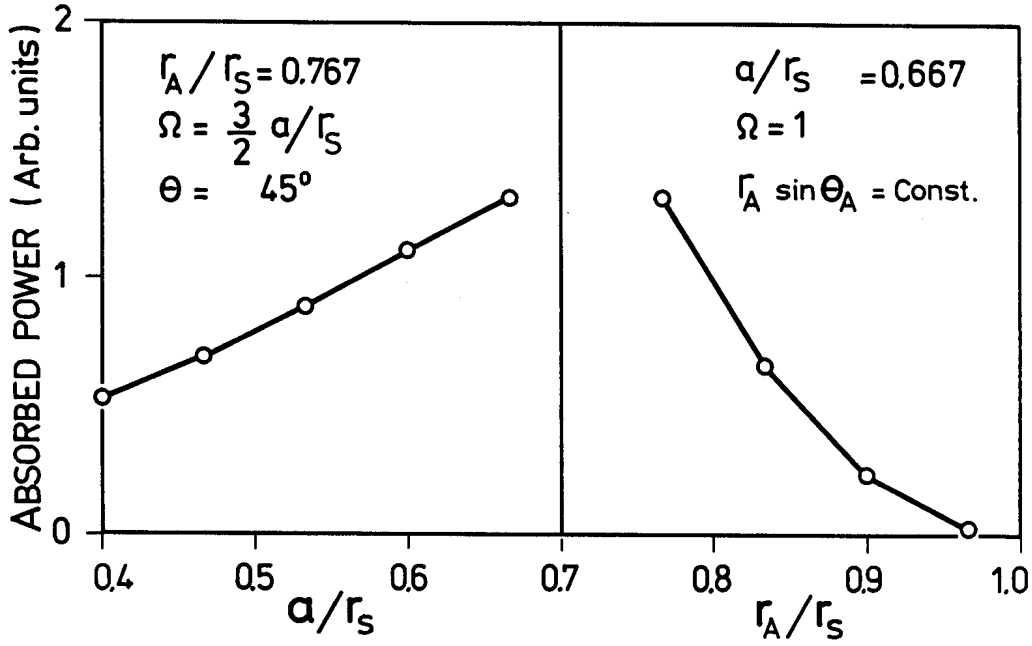
ABSORBED POWER (Arb. units)
2
1
0
$r_A / r_S = 0.767$
$\Omega = \frac{3}{2} a/r_S$
$\theta = 45°$
0.4
0.5
0.6
0.7
a/r_S
$a/r_S = 0.667$
$\Omega = 1$
$r_A \sin\theta_A$ = Const.
0.8
0.9
1.0
r_A/r_S

FIG. 9

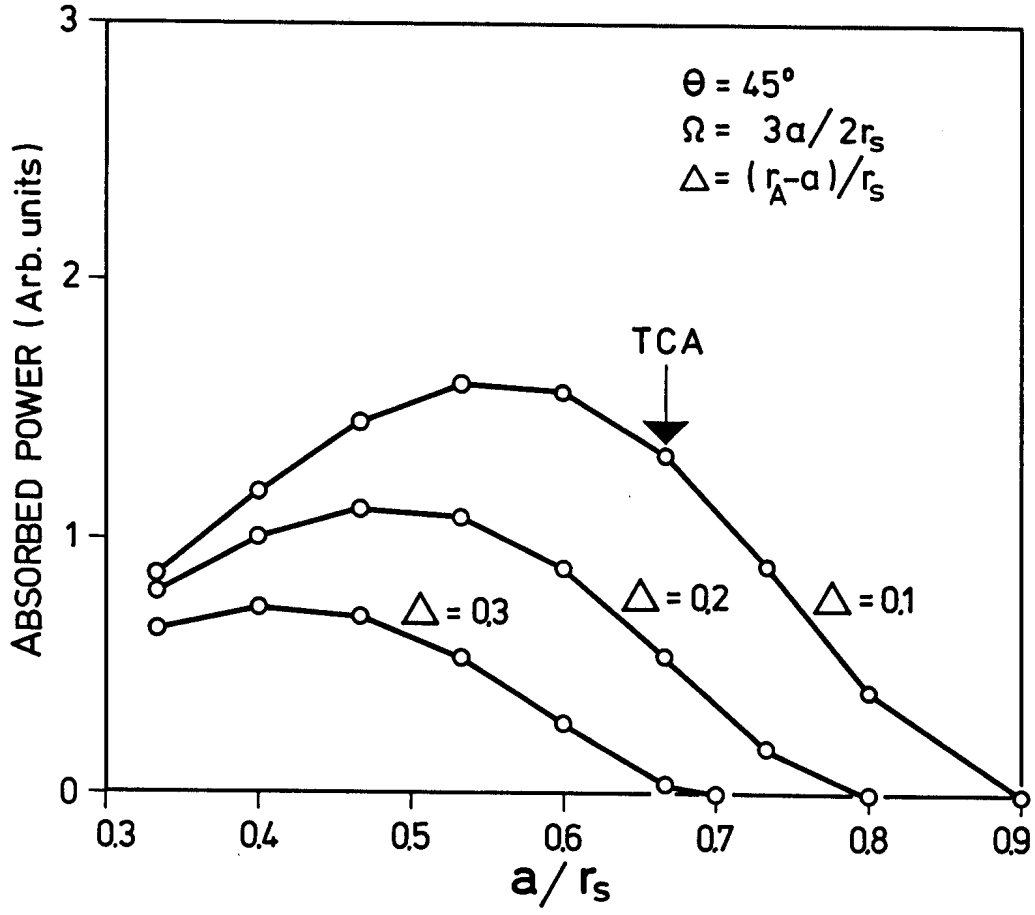
3
2
1
0
ABSORBED POWER (Arb. units)
Θ = 45°
Ω = 3a/2r_s
Δ = (r_A-a)/r_s
TCA
Δ = 0.3
Δ = 0.2
Δ = 0.1
0.3
0.4
0.5
0.6
0.7
0.8
0.9
a/r_s

FIG. 10

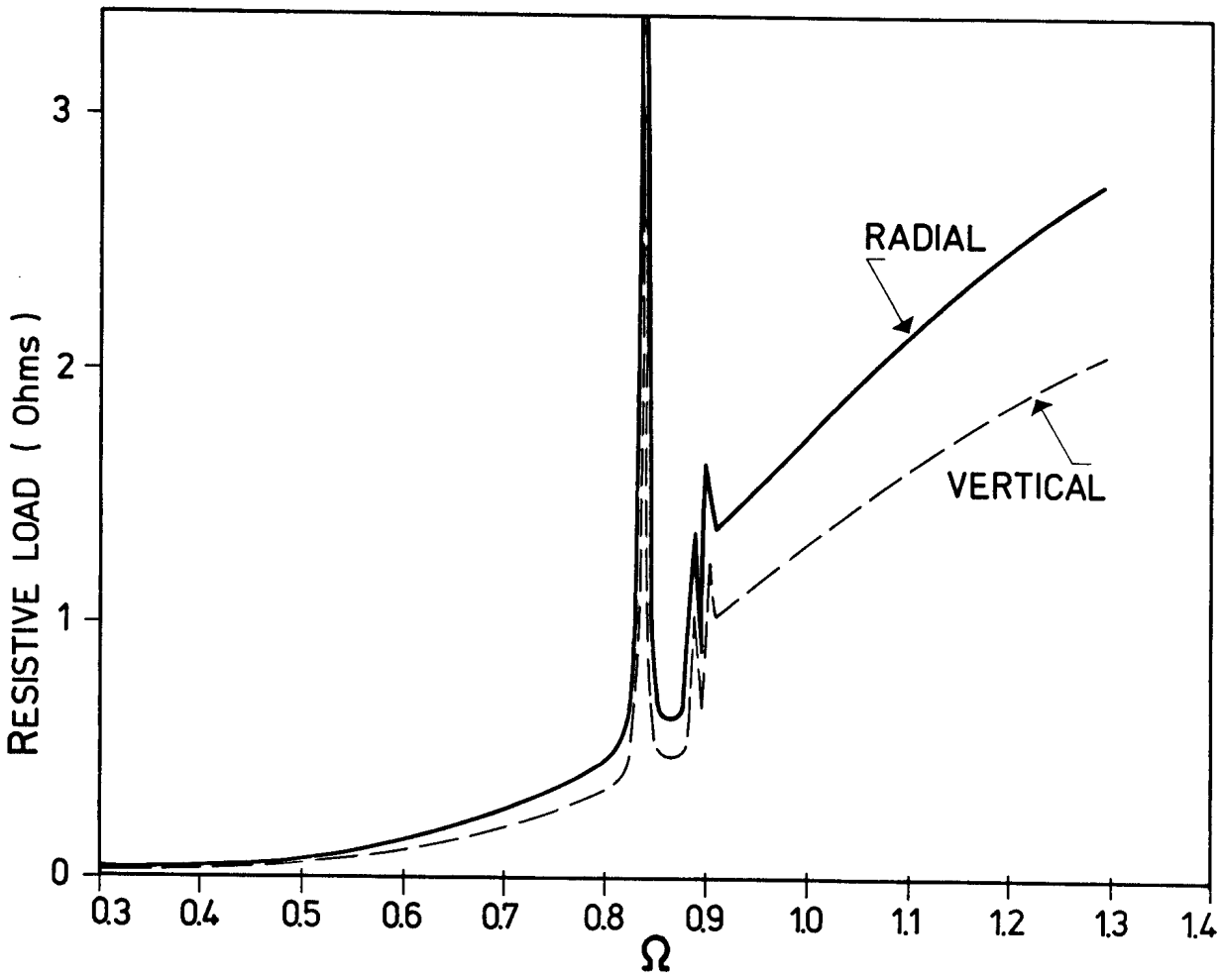
RESISTIVE LOAD (Ohms)
3
2
1
0
RADIAL
VERTICAL
0.3
0.4
0.5
0.6
0.7
0.8
0.9
1.0
1.1
1.2
1.3
1.4
Ω

FIG. 11